

**Authors' final version of a paper  
published in  
"Signal Processing"**

Paper reference:

S. Hosseini, Y. Deville, H. Saylani, "Blind separation of linear instantaneous mixtures of non-stationary signals in the frequency domain", *Signal Processing*, vol. 89, no. 5, pp. 819-830, May 2009.

Elsevier on-line version:

<http://dx.doi.org/10.1016/j.sigpro.2008.10.024>

# Blind separation of linear instantaneous mixtures of non-stationary signals in the frequency domain

Shahram Hosseini <sup>\*,a</sup>, Yannick Deville <sup>a</sup>, Hicham Saylani <sup>a,b</sup>

<sup>a</sup>*Laboratoire d'Astrophysique de Toulouse-Tarbes, Université de Toulouse, CNRS, 14 avenue Edouard Belin - 31400 Toulouse - France.*

<sup>b</sup>*Laboratoire des Systèmes de Télécommunications et Ingénierie de la Décision - Faculté des Sciences - Université Ibn Tofail - 14000 Kénitra - Maroc.*

---

## Abstract

Blind Source Separation (BSS) methods aim at restoring source signals from their mixtures. For linear instantaneous mixtures of *stationary* random sources, a natural and widely used approach consists in using some statistics associated to the *temporal* representation of the signals. On the contrary, we here consider *non-stationary* real sources and we show that they have interesting frequency-domain properties which motivate the introduction of two new frequency-domain BSS methods. The first method works by diagonalizing a zero-lag, second-order statistics matrix, created using both covariance and pseudo-covariance matrices of Fourier transforms of real-valued observations. In practice, this method is specially suitable for separating cyclo-stationary sources. The second method is particularly important because it allows the existing time-domain algorithms developed for stationary, temporally correlated sources (like AMUSE or SOBI) to be extended to non-stationary, temporally uncorrelated sources just by mapping the mixtures into the frequency domain. Both methods set no constraint on the piecewise stationarity of the sources, unlike most previously reported BSS methods exploiting source non-stationarity. The experimental results using artificial and real-world sources confirm the good performance of the proposed methods for non-stationary sources.

*Key words:* Blind source separation, Independent Component Analysis, Non-stationary signals, Cyclo-stationary signals, Covariance and Pseudo-Covariance matrices, Non-circularity.

---

\* Corresponding author, Tel.: +33-5-61-33-28-79; Fax: +33-5-61-33-28-40.  
*Email addresses:* shosseini@ast.obs-mip.fr (Shahram Hosseini), ydeville@ast.obs-mip.fr (Yannick Deville), hsaylani@ast.obs-mip.fr (Hicham Saylani).

## 1 Introduction

Linear instantaneous Blind Source Separation (BSS) consists in recovering unobserved source signals from several observed signals which are supposed to be linear instantaneous mixtures of these sources. It has been shown that this goal can be achieved by exploiting non-gaussianity, time correlation or non-stationarity [1], leading to numerous algorithms (see *e.g.* [2] and references therein).

In this paper, our goal is to propose new approaches using the non-stationarity of the sources. A few authors have studied this problem [3]-[8] using a statistical framework. In [3] and [4], separation of non-stationary signals is achieved using a neural network by cancelling the zero-lag cross-correlation of its outputs at any time point. In [5], the observed signals are divided in two subintervals. Then, the joint diagonalization of two covariance matrices, estimated on the two subintervals, allows one to separate the sources. A somewhat similar algorithm, considering several covariance matrices instead of two, is proposed in [6]. Another approach, presented in [7], is based on the maximization of the non-stationarity, measured by the cross-cumulant, of a linear combination of the observed mixtures. In [8], the authors develop novel approaches based on the principles of maximum likelihood and minimum mutual information.

All the statistical methods mentioned above are *time-domain* methods. Moreover, the estimation of the considered statistics requires that they do not change within some intervals. This means that the non-stationary sources are supposed to be piecewise stationary with respect to the considered statistics, while this hypothesis may not be realistic for many real-world signals.

The statistical methods proposed in the present paper are *frequency-domain* methods. They result from some interesting frequency-domain statistical properties of non-stationary random signals, and may be used for separating linear instantaneous mixtures of Gaussian or non-Gaussian non-stationary, mutually uncorrelated real signals. The first method works by diagonalizing a zero-lag second-order statistics matrix, created using both covariance and pseudo-covariance matrices of Fourier transforms of real-valued observations. In practice, this method is specially suitable for separating cyclo-stationary sources. The second method is particularly important because it allows the existing time-domain algorithms developed for stationary, temporally correlated sources (like AMUSE or SOBI) to be extended to non-stationary, temporally uncorrelated sources just by mapping the mixtures into the frequency domain while theoretically these methods cannot directly be applied to original non-

stationary temporal data, because of the stationarity assumption made by these methods. The piecewise stationarity hypothesis is not required in our proposed methods.

We should mention that statistical frequency-domain methods have been used for separating convolutive mixtures of non-stationary sources (see for example [9]), but in a totally different context which consists in transforming a convolutive time-domain mixture into instantaneous frequency-domain mixtures with frequency-dependent parameters. Moreover, there exist several methods exploiting the time-frequency diversity of non-stationary sources for separating them [10]-[13]. Finally, the FSOBI algorithm proposed in [14] bears a resemblance to one of the algorithms which can be used with our second method, but their algorithm is not motivated by the exploitation of non-stationarity so that the mathematical framework developed in the present paper to achieve our second method is not used by them.

The paper is organized as follows. Section 2 is devoted to problem statement. In Sections 3 and 4, we derive and explain our first and second methods respectively. Experimental results are reported in Section 5. Finally, Section 6 concludes this work. The appendices contain some proofs and other mathematical derivations.

## 2 Problem statement

In a general framework (without noise and with the same number of mixtures and sources), the blind separation of linear instantaneous mixtures can be formulated as follows. Suppose  $N$  samples of  $K$  linear instantaneous mixtures of  $K$  unknown *discrete-time* sources<sup>1</sup> are available. The mixing model is given by

$$\mathbf{x}(n) = \mathbf{A}\mathbf{s}(n) \quad (1)$$

where  $\mathbf{x}(n) = [x_1(n), x_2(n), \dots, x_K(n)]^T$  and  $\mathbf{s}(n) = [s_1(n), s_2(n), \dots, s_K(n)]^T$  are, respectively, the observation and source vectors, and  $\mathbf{A}$  is an *unknown* mixing matrix. In this paper, we suppose the sources are zero-mean, real signals, and the mixing matrix  $\mathbf{A}$  is real and nonsingular. The goal is to find an estimate of the matrix  $\mathbf{A}$  (or its inverse, the separating matrix) up to a permutation and a diagonal matrix. In the following, we suppose also that the components of the source vector  $\mathbf{s}(n)$  in (1), *i.e.* the source signals  $s_i(n)$ ,

---

<sup>1</sup> In this paper, we consider discrete-time signals because in practice one usually deals with such signals. However, it must be emphasized that the methods proposed hereafter can also be used for processing continuous-time signals.

are mutually uncorrelated. In other words, we suppose that  $E[s_i(n_1)s_j(n_2)] = 0 \quad \forall i \neq j, \quad \forall n_1, n_2$ . This hypothesis is weaker than the independence hypothesis, used by many source separation methods.

Let us denote the Fourier transforms<sup>2</sup> of  $s_i(n)$  and  $x_i(n)$  by  $S_i(\omega)$  and  $X_i(\omega)$ , and define  $\mathbf{S}(\omega) = [S_1(\omega), S_2(\omega), \dots, S_K(\omega)]^T$  and  $\mathbf{X}(\omega) = [X_1(\omega), X_2(\omega), \dots, X_K(\omega)]^T$ . Taking the Fourier transform of (1), we obtain

$$\mathbf{X}(\omega) = \mathbf{A}\mathbf{S}(\omega). \quad (2)$$

The uncorrelatedness of the zero-mean sources implies that

$$E[S_i(\omega_1)S_j(\omega_2)] = E[S_i(\omega_1)S_j^*(\omega_2)] = 0 \quad \forall i \neq j, \quad \forall \omega_1, \quad \forall \omega_2 \quad (3)$$

where  $S^*(\omega)$  is the complex conjugate of  $S(\omega)$ . It follows that

**Corollary 1:** The matrices  $\mathbf{Q}_S(\omega) = E[\mathbf{S}(\omega)\mathbf{S}^T(\omega)]$  and  $\mathbf{P}_S(\omega, v) = E[\mathbf{S}(\omega + v)\mathbf{S}^H(\omega)]$  are diagonal for any frequencies  $\omega$  and  $v$ . Here,  $\mathbf{S}^T$  and  $\mathbf{S}^H$  denote, respectively, the transpose and the Hermitian transpose of  $\mathbf{S}$ . For simplifying the notations, we denote  $\mathbf{R}_S(\omega) = \mathbf{P}_S(\omega, 0) = E[\mathbf{S}(\omega)\mathbf{S}^H(\omega)]$ .

According to the terminology used in [16], the matrices  $\mathbf{R}_S(\omega)$  and  $\mathbf{Q}_S(\omega)$  are respectively the covariance and pseudo-covariance matrices of the complex vector  $\mathbf{S}(\omega)$ .

### 3 First method

Our first method is the direct result of the following theorem which makes use of Corollary 1. A Similar version of this theorem has already been demonstrated in [16]. Moreover, similar theorems concerning joint diagonalization of two matrices are well-known and largely used in several source separation algorithms (see for example [17] for AMUSE or [6] for SONS). However, the approach that we use in the following demonstration is somewhat different from that used in the above papers. That's why the proof is provided in the appendix.

---

<sup>2</sup> The Fourier transform of a discrete-time stochastic process  $u(n)$  is a stochastic process  $U(\omega)$  given by  $U(\omega) = \sum_{n=-\infty}^{\infty} u(n)e^{-j\omega n}$ . The equality is interpreted in the mean square sense. See Chapter 11 of [15] for more discussions about statistical properties of this Fourier transform.

**Theorem 1:** Suppose  $s_i(n)$  are  $K$  mutually uncorrelated, zero-mean, real signals. Suppose also there is a frequency  $\omega$  such that  $E[|S_i(\omega)|^2] \neq 0 \forall i$  and

$$\frac{E[S_i^2(\omega)]}{E[|S_i(\omega)|^2]} \neq \frac{E[S_j^2(\omega)]}{E[|S_j(\omega)|^2]}, \quad \forall i \neq j. \quad (4)$$

Define  $\mathbf{R}_X(\omega) = E[\mathbf{X}(\omega)\mathbf{X}^H(\omega)]$  and  $\mathbf{Q}_X(\omega) = E[\mathbf{X}(\omega)\mathbf{X}^T(\omega)]$ . If  $\mathbf{V}$  is a matrix whose columns are the eigenvectors of  $\mathbf{R}_X^{-1}(\omega)\mathbf{Q}_X(\omega)$ , *i.e.* if

$$\mathbf{R}_X^{-1}(\omega)\mathbf{Q}_X(\omega) = \mathbf{V}\mathbf{\Lambda}\mathbf{V}^{-1} \quad (5)$$

where  $\mathbf{\Lambda}$  is a diagonal matrix, then  $\mathbf{V}^T = \mathbf{P}\mathbf{D}\mathbf{A}^{-1}$ , where  $\mathbf{D}$  is a complex diagonal matrix and  $\mathbf{P}$  is a permutation matrix.

Conversely, if  $\exists i \neq j$  such that  $\frac{E[S_i^2(\omega)]}{E[|S_i(\omega)|^2]} = \frac{E[S_j^2(\omega)]}{E[|S_j(\omega)|^2]}$  for a given frequency  $\omega$ , then the eigenvalue decomposition (5) at  $\omega$  does not give the matrix  $\mathbf{A}^{-1}$  up to a permutation and a diagonal matrix<sup>3</sup>.

*Proof:* See Appendix A.

According to Theorem 1, if the identifiability condition (4) is satisfied for a given frequency  $\omega_1$ , then the eigenvalue decomposition of  $\mathbf{R}_X^{-1}(\omega_1)\mathbf{Q}_X(\omega_1)$  gives a matrix  $\mathbf{V}$  such that its transpose,  $\mathbf{V}^T$ , is equal to the separating matrix  $\mathbf{A}^{-1}$  up to a permutation and a complex diagonal matrix. Since  $\mathbf{A}$  is supposed to be real, we should take the real part of the matrix  $\mathbf{V}^T$ . In fact, writing  $\mathbf{V}^T = \mathbf{P}\mathbf{D}\mathbf{A}^{-1} = \mathbf{P}(\mathbf{D}_R + j\mathbf{D}_I)\mathbf{A}^{-1}$  where  $\mathbf{D} = \mathbf{D}_R + j\mathbf{D}_I$  is a complex diagonal matrix with real and imaginary parts  $\mathbf{D}_R$  and  $\mathbf{D}_I$ , it is clear that  $\Re\{\mathbf{V}^T\} = \mathbf{P}\mathbf{D}_R\mathbf{A}^{-1}$  *i.e.* the separating matrix  $\mathbf{A}^{-1}$  is equal to the real part of the matrix  $\mathbf{V}^T$  up to a permutation and a *real* diagonal matrix. Then, the sources may be estimated, up to a permutation and a real scaling factor, using the following equation

$$\Re\{\mathbf{V}^T\}\mathbf{x}(n) = \mathbf{P}\mathbf{D}_R\mathbf{A}^{-1}\mathbf{x}(n) = \mathbf{P}\mathbf{D}_R\mathbf{s}(n). \quad (6)$$

We now show that, as a specific consequence of Theorem 1, the proposed method does not work if the mixtures contain more than one stationary source. We begin by the following proposition.

**Proposition 1:** Let  $s(n)$  be a real stationary signal with Fourier transform  $S(\omega)$ . Then,  $E[S^2(\omega)] = 0$  for  $\omega \neq k\pi$  where  $k$  is an integer.

<sup>3</sup> Note that if the Fourier transforms of the real signals  $s_i(n)$  are circular, they do not satisfy Condition (4). The BSS approach that we will derive from this theorem therefore applies to signals whose frequency-domain representations are non-circular.

*Proof:* This proposition may be easily proved using the materials provided in Chapter 11 of [15] (see in particular Page 515).

It follows that:

**Theorem 2:** If  $s_i(n)$  and  $s_j(n)$  are two real stationary sources, then for any frequency  $\omega$

$$\frac{E[S_i^2(\omega)]}{E[|S_i(\omega)|^2]} = \frac{E[S_j^2(\omega)]}{E[|S_j(\omega)|^2]} \quad (7)$$

*Proof:* Considering Proposition 1, it is clear that for two real stationary sources  $s_i(n)$  and  $s_j(n)$ , (7) holds for  $\omega \neq k\pi$  because its two sides are equal to zero. Moreover, since the Fourier transform of a real signal is real at  $\omega = k\pi$  (because  $e^{-jk\pi n}$  is real), we can write  $E[S_i^2(k\pi)] = E[|S_i(k\pi)|^2]$  so that the two sides of (7) are equal to one for  $\omega = k\pi$ .

Theorems 1 and 2 imply that if the mixtures contain at least two stationary sources, they cannot be completely separated at any frequency  $\omega$ . Hence, a necessary condition for applying the method is that at most one of the sources be stationary.

**Discussion:** Considering (5) and the definitions of the matrices  $\mathbf{R}_X(\omega)$  and  $\mathbf{Q}_X(\omega)$ , the implementation of the proposed BSS method requires one to estimate the expected values of some frequency-domain functions. Three different cases may be considered.

a) Several realizations of the mixtures  $x_i(n)$  are available. In this case, the expected values may be approximated by averaging the frequency-domain functions on these realizations (for a particular frequency). Unfortunately, this case may rarely occur in practice.

b) Only one realization of the mixtures is available but the frequency-domain functions are ergodic so that the expected values can be estimated by frequency averages. A necessary condition for the ergodicity is the stationarity of the frequency-domain functions, *i.e.*, the expected values used in the definitions of  $\mathbf{R}_X(\omega)$  and  $\mathbf{Q}_X(\omega)$  must not depend on  $\omega$ . However, it seems difficult to guarantee this condition for most real-world signals. For example, we will show in Theorem 3 that if the sources are cyclo-stationary,  $\mathbf{Q}_X(\omega)$  is nonzero only for certain values of  $\omega$  so that it is not stationary.

c) Only one realization of the mixtures is available but the mixtures are cyclo-stationary so that each cyclo-stationarity period may be considered itself as a

separate realization of the stochastic process  $x_i(n)$ . In this case, by splitting the mixtures in several time frames, each one containing an integral number of cyclo-stationarity periods, we obtain several realizations of the mixtures which may be used for estimating the expected values. This case is more realistic than the previous two, and will be considered in the following. For example, in the radiocommunications context, the sources resulting from digital modulation are very often cyclo-stationary [19] and their blind separation has already been considered in the literature [20]-[22].

**Algorithm:** For the case of cyclo-stationary sources, the proposed algorithm may be summarized as follows.

- (1) Split the mixed signals  $x_i(n)$  in  $L$  frames  $x_{i,l}(n)$ ,  $l = 1, \dots, L$ . The choice of  $L$  will be discussed further.
- (2) Take the Fourier transform of each frame  $x_{i,l}(n)$  to obtain  $X_{i,l}(\omega)$   $l = 1, \dots, L$ .
- (3) For each frame  $l$ , form a matrix  $\mathbf{X}_l(\omega) = [X_{1,l}(\omega), X_{2,l}(\omega), \dots, X_{K,l}(\omega)]^T$  containing the Fourier transforms of all the observations in that frame.
- (4) Compute the estimated matrices  $\hat{\mathbf{R}}_X(\omega)$  and  $\hat{\mathbf{Q}}_X(\omega)$  by averaging  $\mathbf{X}_l(\omega)\mathbf{X}_l^H(\omega)$  and  $\mathbf{X}_l(\omega)\mathbf{X}_l^T(\omega)$  over all  $L$  frames:  $\hat{\mathbf{R}}_X(\omega) = \frac{1}{L} \sum_{l=1}^L \mathbf{X}_l(\omega)\mathbf{X}_l^H(\omega)$ ,  $\hat{\mathbf{Q}}_X(\omega) = \frac{1}{L} \sum_{l=1}^L \mathbf{X}_l(\omega)\mathbf{X}_l^T(\omega)$ .
- (5) Choose a frequency  $\omega_1$  where the conditions of Theorem 1 are hoped to be met. This issue will be discussed further.
- (6) Find the eigenvectors of the matrix  $\hat{\mathbf{R}}_X^{-1}(\omega_1)\hat{\mathbf{Q}}_X(\omega_1)$ . Form a matrix  $\hat{\mathbf{V}}$  whose columns are these eigenvectors.
- (7) Obtain an estimate of the separating matrix using  $\hat{\mathbf{A}}^{-1} = \Re\{\hat{\mathbf{V}}^T\}$ .

Steps 1 and 5 require some comments. If the source cyclo-stationarity periods  $N_{c_i}$  are integers, then the observations are cyclo-stationary too and their common cyclo-stationary period is equal to the least common multiplier of  $N_{c_i}$ . Thus, one should preferably choose the frames such that each frame contains an integral number of this common period. If  $N_{c_i}$  are not known, the common cyclo-stationary period may be estimated from observations using some preprocessing [22], [23]. If  $N_{c_i}$  are not integers, acceptable results may be obtained by choosing the frames such that each of them contains a great number of source cyclo-stationarity periods because the last incomplete periods have a negligible influence on the parameter values obtained by time averaging. In the following, we suppose the data are sampled such that  $N_{c_i}$  are integers. The choice of the frequency  $\omega_1$  in Step 5 is another important issue. The following theorem and its corollary provide necessary conditions for choosing this frequency.

**Theorem 3:** If  $s(n)$  is a cyclo-stationary signal with cyclo-stationarity fre-



quency  $\omega_c = \frac{2\pi}{N_c}$ , where  $N_c$  is the cyclo-stationarity period, then  $E[S^2(\omega)] = 0$  everywhere except, possibly, at frequencies  $\omega = k\omega_c/2$  where  $k$  is an integer.

*Proof:* See Appendix B.

**Corollary 2:** Given  $N$  cyclo-stationary sources  $s_i(n)$  with cyclo-stationarity frequencies  $\omega_{c_i}$ , the identifiability condition (4) cannot be satisfied except, possibly, at frequencies  $\omega = k\omega_l/2$ , where  $k$  is an integer and  $\omega_l$  is the least common multiplier of  $N - 1$  source cyclo-stationarity frequencies<sup>4</sup>. Moreover, the identifiability condition is not satisfied at  $\omega = k\pi$ .

*Proof:* Following Theorem 3, if  $\omega \neq k\omega_l/2$ , then  $E[S_i^2(\omega)] = 0$  at least for two different values of  $i$ , such that the identifiability condition (4) is not satisfied. Moreover, as mentioned in the proof of Theorem 2, the identifiability condition does not hold at  $\omega = k\pi$  because the two sides of (4) are equal to one.

Note that the above corollary proposes us a set of possible candidates for choosing  $\omega_1$  but does not specify which of them must be chosen. This problem is not specific to our method. In fact, all the source separation algorithms based on eigenvalue decomposition have similar difficulties to guarantee the existence of distinct eigenvalues, required for satisfying some identifiability conditions.

The analysis of the entries of the matrix  $\mathbf{Q}_X(\omega)$  may give us some indications on the good choices for  $\omega_1$ . Following the above discussion, the frequencies at which the entries of this matrix are zero should be avoided because it is possible that  $E[S_i^2(\omega)] = 0 \quad \forall i$  at these frequencies. A good idea may be to choose the (non-multiple of  $\pi$ ) frequencies at which the entries have great absolute values.

As used in some classical time-domain source separation algorithms (see for example [24]), it is also possible to choose some linear combinations  $\sum_i \sum_k \alpha_{ik} \mathbf{R}_X^{-1}(k\omega_{l_i}/2) \mathbf{Q}_X(k\omega_{l_i}/2)$  instead of only one frequency, or to jointly diagonalize several matrices  $\mathbf{R}_X^{-1}(k\omega_{l_i}/2) \mathbf{Q}_X(k\omega_{l_i}/2)$  for different values of  $k$  and  $i$ . Then, it is sufficient that the identifiability condition (4) is satisfied for one of these frequencies.

---

<sup>4</sup> It can be verified that  $\omega_l = 2\pi/N_l$  where  $N_l$  is the greatest common divisor of  $N - 1$  source cyclo-stationarity periods. Since  $N$  different combinations of  $N - 1$  sources among  $N$  may be considered,  $N$  different values for  $\omega_l$  may be obtained.

## 4 Second method

Our second method is based on the following theorem.

**Theorem 4:** If  $s(n)$  is a temporally uncorrelated, real, zero-mean signal with a (possibly non-stationary) variance  $\gamma(n)$ , *i.e.* if  $E[s(n_1)s(n_2)] = \gamma(n_1)\delta(n_1-n_2)$ , where  $\delta(n)$  is the unit impulse, then its Fourier transform,  $S(\omega)$  is a wide-sense stationary process with autocorrelation  $\Gamma(v)$ , which is the Fourier transform of  $\gamma(n)$ , *i.e.*

$$E[S(\omega + v)S^*(\omega)] = \Gamma(v) = \sum_{n=-\infty}^{\infty} \gamma(n)e^{-jvn}. \quad (8)$$

Moreover, if  $s(n)$  is non-stationary with respect to its variance  $\gamma(n)$ , *i.e.* if  $\gamma(n)$  is not constant, then the process  $S(\omega)$  is autocorrelated.

*Proof:* This theorem may be easily proved using the materials provided in Chapter 11 of [15], and in particular Theorem 11-2 of this chapter.

Hence, if we suppose that the mutually uncorrelated sources  $s_i(n)$  are real, zero-mean, temporally uncorrelated and non-stationary with respect to their variances, then Equations (2) and (3) and Theorem 4 entail that  $X_i(\omega)$  are linear mixtures of mutually uncorrelated, wide-sense stationary and autocorrelated processes  $S_i(\omega)$ . Many algorithms have been proposed for separating such mixtures [17], [24]-[26]. Although these algorithms were originally developed for time-domain wide-sense stationary, time-correlated processes, nothing prohibits us from applying them to frequency-domain wide-sense stationary, frequency-correlated processes. Thus, only by mapping the non-stationary temporally uncorrelated observed signals in the frequency domain, source separation can be achieved using one of the numerous methods developed previously for time-correlated stationary sources<sup>5</sup>.

We here propose such an algorithm, which may be considered as a modified frequency-domain version of the time-domain AMUSE algorithm [17]<sup>6</sup>. It consists in diagonalizing the matrix  $\mathbf{R}_X(\omega)^{-1}\mathbf{P}_X(\omega, v_1)$  for some frequency shift

<sup>5</sup> Note that our method is based on second-order statistical properties of the Fourier transform of random processes, and not based on the Fourier transform of second-order statistical properties of temporal signals (like Power Spectral Density).

<sup>6</sup> We emphasize that this algorithm is just an example, chosen for its simplicity of implementation. The principal advantage of our second method is that it can be used to “adapt” every algorithm developed for time-correlated stationary sources to non-stationary temporally uncorrelated sources.

$v_1$ , where  $\mathbf{R}_X(\omega) = E[\mathbf{X}(\omega)\mathbf{X}^H(\omega)]$  and  $\mathbf{P}_X(\omega, v_1) = E[\mathbf{X}(\omega + v_1)\mathbf{X}^H(\omega)]$ . The diagonalization may be achieved using eigenvalue decomposition as the following theorem suggests.<sup>7</sup>

**Theorem 5:** Suppose  $s_i(n)$  are  $K$  mutually uncorrelated zero-mean real signals. Suppose also there exists a frequency  $\omega$  and a frequency shift  $v_1$  such that  $E[|S_i(\omega)|^2] \neq 0 \forall i$  and

$$\frac{E[S_i(\omega + v_1)S_i^*(\omega)]}{E[|S_i(\omega)|^2]} \neq \frac{E[S_j(\omega + v_1)S_j^*(\omega)]}{E[|S_j(\omega)|^2]} \quad \forall i \neq j. \quad (9)$$

If  $\mathbf{V}$  is a matrix whose columns are the eigenvectors of  $\mathbf{R}_X(\omega)^{-1}\mathbf{P}_X(\omega, v_1)$ , *i.e.* if

$$\mathbf{R}_X(\omega)^{-1}\mathbf{P}_X(\omega, v_1) = \mathbf{V}\mathbf{\Lambda}\mathbf{V}^{-1} \quad (10)$$

where  $\mathbf{\Lambda}$  is a diagonal matrix, then  $\mathbf{V}^T = \mathbf{P}\mathbf{D}\mathbf{A}^{-1}$ , where  $\mathbf{D}$  is a complex diagonal matrix and  $\mathbf{P}$  is a permutation matrix. It follows that  $\Re\{\mathbf{V}^T\} = \mathbf{P}\mathbf{D}_R\mathbf{A}^{-1}$  where  $\mathbf{D}_R$  is a real diagonal matrix.

Conversely, if  $\exists i \neq j$  such that

$$\frac{E[S_i(\omega + v_1)S_i^*(\omega)]}{E[|S_i(\omega)|^2]} = \frac{E[S_j(\omega + v_1)S_j^*(\omega)]}{E[|S_j(\omega)|^2]} \quad (11)$$

for a given frequency  $\omega$  and a frequency shift  $v_1$ , then the eigenvalue decomposition (10) at  $\omega$  and  $v_1$  does not give the matrix  $\mathbf{A}^{-1}$  up to a permutation and a diagonal matrix.

*Proof:* The proof is similar to that of Theorem 1 by replacing the appropriate matrices, and noting from Corollary 1 that the matrices  $\mathbf{R}_S(\omega)$  and  $\mathbf{P}_S(\omega, v_1)$  are diagonal.

Following Theorem 4, if two sources  $s_i(n)$  and  $s_j(n)$  are temporally uncorrelated, real, zero-mean signals with variances  $\gamma_i(n)$  and  $\gamma_j(n)$ , then the numerators and the denominators in (9) are the Fourier transforms of these variances ( $\Gamma_i(v)$  and  $\Gamma_j(v)$ ) at the frequencies  $v = v_1$  and  $v = 0$ . Thus, Theorem 5 shows that the  $K$  sources may be separated if and only if they have different normalized variance profiles.

We now show that the proposed method is not able to separate two stationary sources. Since the variance profile of a stationary source  $s_i(n)$  is constant (*i.e.*  $\gamma_i(n) = \gamma_i$ ), its Fourier transform (which is equal to  $\Gamma(v) = E[S_i(\omega + v)S_i^*(\omega)]$ ,

<sup>7</sup> This theorem is similar to that used in the AMUSE algorithm [17].

due to Theorem 4) is zero everywhere except at<sup>8</sup>  $v = 2k\pi$ . Moreover, at  $v = 2k\pi$ , we have  $E[S_i(\omega + v)S_i^*(\omega)] = E[|S_i(\omega)|^2]$ . Hence, if  $s_i(n)$  and  $s_j(n)$  are two stationary sources, we can write

$$\frac{E[S_i(\omega + v_1)S_i^*(\omega)]}{E[|S_i(\omega)|^2]} = \frac{E[S_j(\omega + v_1)S_j^*(\omega)]}{E[|S_j(\omega)|^2]} = \begin{cases} 1 & \text{if } v_1 = 2k\pi \\ 0 & \text{if } v_1 \neq 2k\pi \end{cases} \quad (12)$$

Theorem 5 then implies that two stationary sources cannot be separated. Therefore, a necessary condition for applying the method is that at most one of the sources is stationary.

Since the processes  $S_i(\omega)$  and therefore  $X_i(\omega)$  are wide-sense stationary in the considered conditions, we can hope they are also wide-sense ergodic, so that the expected values involved in  $\mathbf{R}_X(\omega)$  and  $\mathbf{P}_X(\omega, v_1)$  can be estimated by frequency averages. Thus, if  $X_i(\omega)$  are evaluated for  $N$  frequencies  $\omega_n = \frac{2\pi n}{N}$ , we can write<sup>9</sup>  $\hat{\mathbf{R}}_X = \frac{1}{N} \sum_{n=0}^{N-1} \mathbf{X}(\omega_n)\mathbf{X}^H(\omega_n)$  and  $\hat{\mathbf{P}}_X(v_1) = \frac{1}{N} \sum_{n=0}^{N-1} \mathbf{X}(\omega_n + v_1)\mathbf{X}^H(\omega_n)$ . In this case, the proposed BSS algorithm reduces to the eigenvalue decomposition of the sample matrix  $\hat{\mathbf{R}}_X^{-1}\hat{\mathbf{P}}_X(v_1)$ .

Note also that, as in the time-domain algorithms, the estimation algorithm may be split in two steps, *i.e.* by first whitening data which is equivalent to diagonalizing  $\mathbf{R}_X(\omega)$  and then by computing  $\mathbf{P}_X(\omega, v_1)$  on the whitened data and diagonalizing it using a unitary matrix.

Like with our first method and the other source separation algorithms based on eigenvalue decomposition, it is difficult to guarantee identifiability. Here, there is no way to choose the frequency shift  $v_1$  so that identifiability is ensured. In practice,  $v_1$  may be chosen by examining the entries of the matrix  $\mathbf{P}_X(\omega, v_1)$ . The frequency shifts at which the entries of this matrix are zero should be avoided because it is possible that  $E[S_i(\omega + v_1)S_i^*(\omega)] = 0 \quad \forall i$  at these frequency shifts so that (9) is not satisfied. A good idea to avoid these frequencies may be to choose a value of  $v_1$  for which the entries of  $\mathbf{P}_X(\omega, v_1)$  have great absolute values. A better solution, which can be considered as a frequency-domain counterpart of the SOBI algorithm [24], is to simultaneously diagonalize several matrices  $\mathbf{R}_X(\omega)^{-1}\mathbf{P}_X(\omega, v)$  corresponding to several frequency shifts  $v$ . Then, it is enough that the identifiability condition (9) is satisfied for one of these frequency shifts. Thus, the choice of  $v$  is a somewhat less serious problem.

<sup>8</sup> The discrete-time Fourier transform of a constant  $\gamma_i$  is equal to  $2\pi\gamma_i \sum_{k=-\infty}^{\infty} \delta(v - 2k\pi)$ .

<sup>9</sup> Note that since  $X_i(\omega)$  are stationary, the covariance matrices  $\mathbf{R}_X(\omega)$  and  $\mathbf{P}_X(\omega, v_1)$  do not depend on  $\omega$ .

## Case of autocorrelated sources

The second method proposed in this section supposes that the considered sources are temporally uncorrelated. In fact, following Theorem 4, the uncorrelatedness of sources is a necessary condition in order that their Fourier transforms be stationary and autocorrelated. This assumption may seem too restrictive because a great number of real-world sources are autocorrelated. We here propose an approach to cope with this problem. This approach is based on the following theorem.

**Theorem 6:** Let  $s_i(n)$   $i = 1, \dots, K$  be  $K$  autocorrelated, real, zero-mean, mutually uncorrelated random signals. Suppose  $z(n)$  is a temporally uncorrelated, stationary random signal, independent from  $s_i(n) \forall i$ . Then, the signals  $\tilde{s}_i(n) = z(n)s_i(n)$   $i = 1, \dots, K$  are temporally and mutually uncorrelated. Moreover, each new source  $\tilde{s}_i(n)$  has the same normalized variance profile as the original source  $s_i(n)$ .

*Proof:* See Appendix C.

Our approach for autocorrelated sources consists in multiplying all the observed signals  $x_i(n)$   $i = 1, \dots, K$  by an arbitrary stationary, temporally uncorrelated random signal  $z(n)$  which is independent from all the source signals  $s_i(n)$   $i = 1, \dots, K$ . Then, we can form a new observation vector  $\tilde{\mathbf{x}}(n)$  whose components are the resulting signals  $\tilde{x}_i(n) = z(n)x_i(n)$ . It is clear that

$$\tilde{\mathbf{x}}(n) = z(n)\mathbf{x}(n) = z(n)\mathbf{A}\mathbf{s}(n) = \mathbf{A}\tilde{\mathbf{s}}(n) \quad (13)$$

where  $\tilde{\mathbf{s}}(n) = [\tilde{s}_1(n), \dots, \tilde{s}_K(n)]^T$  and  $\tilde{s}_i(n) = z(n)s_i(n)$   $i = 1, \dots, K$ . Following Equation (13), the new observations  $\tilde{x}_i(n)$  are linear instantaneous mixtures of the new sources  $\tilde{s}_i(n)$ . Since the new sources are temporally uncorrelated, they verify the condition of Theorem 4. Thus, we can apply the second method to the new observations to estimate the inverse of the mixing matrix  $\mathbf{A}$  and then the original sources  $s_i(n)$  by inverting Equation (1). Note that if the original sources satisfy the identifiability condition (9), the new sources  $\tilde{s}_i(n)$  satisfy it too because, following Theorem 6, they preserve their normalized variance profiles after multiplication by  $z(n)$ .

## 5 Experimental results

In this section, we present our experimental results using artificial and real-world sources.

### 5.1 Results using two artificial sources

In the first experiment, we consider the following non-stationary signals:  $s_1(n) = \mu_1(n)g_1(n)$ ,  $s_2(n) = \mu_2(n)g_2(n)$ , where  $g_1(n)$  and  $g_2(n)$  are mutually independent Gaussian i.i.d. signals with zero mean and unit variance,  $\mu_1(n) = 2\cos(\omega_0 n)$ , and  $\mu_2(n) = 2\sin(\omega_0 n)$ . The mixing matrix is  $\mathbf{A} = \begin{pmatrix} 1 & 0.9 \\ 0.8 & 1 \end{pmatrix}$ , which corresponds to a highly-mixed model.

#### 5.1.1 Results using the first method

In the first step, we want to separate these sources using the method proposed in Section 3. It can be easily shown (see Appendix D) that for these sources

$$\begin{aligned} E[S_1^2(\omega)] &= 2\pi \sum_{l=-\infty}^{\infty} 2\delta(2\omega - 2l\pi) + \delta(2\omega - 2\omega_0 - 2l\pi) + \delta(2\omega + 2\omega_0 - 2l\pi) \\ E[S_2^2(\omega)] &= 2\pi \sum_{l=-\infty}^{\infty} 2\delta(2\omega - 2l\pi) - \delta(2\omega - 2\omega_0 - 2l\pi) - \delta(2\omega + 2\omega_0 - 2l\pi), \end{aligned} \tag{14}$$

which is consistent with Theorem 3, as shown in Appendix D.

Since  $E[S_1^2(\omega)]$  and  $E[S_2^2(\omega)]$  highly depend on  $\omega$ , they cannot be estimated by frequency averages. However, as  $s_1(n)$  and  $s_2(n)$  are cyclo-stationary, we can estimate the expected values using the method proposed in part (c) of the discussion of Section 3.

The experiment was done using 1 second of the sources  $s_1(n)$  and  $s_2(n)$  containing 8192 samples. The frequency  $\omega_0 = \pi/8$  was chosen so that each period of  $\mu_1(n)$  and  $\mu_2(n)$  contains 16 points. Hence, the signals  $s_1(n)$  and  $s_2(n)$  include 512 periods of  $\mu_1(n)$  and  $\mu_2(n)$ . Then, the 16-point Discrete Fourier Transforms of the mixtures  $x_1(n)$  and  $x_2(n)$  were computed on each of 512 frames of 1 period. The spectral expected values were estimated by averaging the spectral functions on these 512 frames. Figure 1 shows the estimates of

$E[S_1^2(\omega)]$  and  $E[S_2^2(\omega)]$ , which are in agreement with the theoretical values of Equations (14). From this figure, it is clear that  $E[S_1^2(\omega)] = E[S_2^2(\omega)] = 0$  everywhere except at  $\omega = l\pi$  and  $\omega = l\pi \pm \omega_0$ . Moreover, considering the argument used in the proof of Theorem 2, at  $\omega = l\pi$  we have  $\frac{E[S_1^2(\omega)]}{E[|S_1(\omega)|^2]} = \frac{E[S_2^2(\omega)]}{E[|S_2(\omega)|^2]} = 1$ . Hence, the only frequencies at which condition (4) of Theorem 1 may hold are  $\omega = l\pi \pm \omega_0$ . Choosing  $\omega_1 = \omega_0$ , we can now apply the algorithm described in Section 3.

The experiment was repeated 100 times corresponding to 100 different seed values of the random variable generator. For each experiment, the output Signal to Interference Ratio (in dB), averaged on  $K = 2$  channels, was computed by

$$SIR = \frac{1}{K} \sum_{i=1}^K 10 \log_{10} \frac{E[s_i^2]}{E[(\hat{s}_i - s_i)^2]}, \quad (15)$$

after normalizing the estimated sources,  $\hat{s}_i(n)$ , so that they have the same variances as the source signals,  $s_i(n)$ . The mean and the standard deviation of SIR on the 100 experiments were 35.4 dB and 7.2 dB.

Other experiments in the same conditions but using other mixing matrices led to similar results. For example, using the mixing matrix  $\mathbf{A} = \begin{pmatrix} 1 & 0.4 \\ 0.3 & 1 \end{pmatrix}$ , the mean and the standard deviation of SIR were 35.4 dB and 7.1 dB. Therefore, the algorithm is robust to the variations of the mixing matrix. The running time of the algorithm implemented in the Matlab language on a Pentium 4 PC was 0.019 sec for each experiment.

### 5.1.2 Results using the second method

In the second step, we want to separate the same sources using the method proposed in Section 4. This time, we compute the Fourier transforms of  $x_1(n)$  and  $x_2(n)$  on the whole signals. The theoretical autocorrelation functions of  $S_1(\omega)$  and  $S_2(\omega)$  are equal to (see Appendix E)

$$\begin{aligned} E[S_1(\omega + v)S_1^*(\omega)] &= 2\pi \sum_{l=-\infty}^{\infty} 2\delta(v - 2l\pi) + \delta(v - 2\omega_0 - 2l\pi) + \delta(v + 2\omega_0 - 2l\pi) \\ E[S_2(\omega + v)S_2^*(\omega)] &= 2\pi \sum_{l=-\infty}^{\infty} 2\delta(v - 2l\pi) - \delta(v - 2\omega_0 - 2l\pi) - \delta(v + 2\omega_0 - 2l\pi) \end{aligned} \quad (16)$$

An experimental estimate of the autocorrelation function of  $S_1(\omega)$  with the parameters used in the first step is shown in Figure 2 which confirms the theoretical result (16). In our experiment, a biased estimator (whose variance is smaller than that of an unbiased estimator) was used for estimating the autocorrelation function. The biased estimator has a tendency to attenuate far lags because less amount of data is available for estimating these lags. That is why the peaks at  $2\pi \pm 2\omega_0$  are smaller than the peaks at  $\pm 2\omega_0$ .

Note that  $E[S_1(\omega + v)S_1^*(\omega)] = E[S_2(\omega + v)S_2^*(\omega)] = 0$  everywhere except at  $v = 2l\pi$  and  $v = 2l\pi \pm 2\omega_0$ . Moreover, at  $v = 2l\pi$  we have  $\frac{E[S_1(\omega+v)S_1^*(\omega)]}{E[|S_1(\omega)|^2]} = \frac{E[S_2(\omega+v)S_2^*(\omega)]}{E[|S_2(\omega)|^2]} = 1$ . Hence, the only frequency shifts at which condition (9) of Theorem 5 may hold are  $v = 2l\pi \pm 2\omega_0$ . The separating matrix may be estimated by applying the method defined in Section 4 choosing  $v_1 = 2\omega_0$ .

We used the modified frequency-domain version of the AMUSE algorithm mentioned in Section 4 for this purpose. Using the same signals as in the first step and  $\mathbf{A} = \begin{pmatrix} 1 & 0.9 \\ 0.8 & 1 \end{pmatrix}$ , the mean and the standard deviation of SIR were 49.4 dB and 5.9 dB.

Other experiments in the same conditions but using other mixing matrices led to similar results. For example, using the mixing matrix  $\mathbf{A} = \begin{pmatrix} 1 & 0.4 \\ 0.3 & 1 \end{pmatrix}$ , the mean and the standard deviation of SIR were also 49.4 dB and 5.9 dB. Therefore, the algorithm is robust to the variations of the mixing matrix. The running time of the algorithm implemented in the Matlab language on a Pentium 4 PC was 0.062 sec for each experiment.

### 5.1.3 Results using other source separation algorithms

Now, we want to separate the same sources as above using the 19 classical algorithms provided by the Matlab toolbox ICALAB 2.2 available at [27]. One can find links towards references concerning the considered algorithms in the *Help* included in this package. Our second method outperforms all 19 algorithms. Our first method is outperformed only by two algorithms: ThinICA (mean of SIR=47.3 dB, standard deviation=5.8 dB) and FPICA (mean of SIR=37.0 dB, standard deviation=16.8 dB).

Other experiments with different profiles of non-stationary variance for the sources  $s_1(n)$  and  $s_2(n)$  led to similar results.



## 5.2 Results using more than 2 artificial sources

In the following, we want to evaluate the performance of our methods as a function of the number  $K$  of sources and mixtures. The considered sources are the signals  $s_1(n)$  and  $s_2(n)$  presented in the previous subsection and two other sources  $s_3(n)$  and  $s_4(n)$  obtained by multiplying mutually independent, Gaussian i.i.d. signals respectively by a sawtooth signal and a symmetrical triangular signal with the same frequency as  $\mu_1(n)$  and  $\mu_2(n)$ .

At first, we consider the 3 sources  $s_1(n)$ ,  $s_2(n)$  and  $s_3(n)$ , mixed by the matrix

$$\mathbf{A} = \begin{pmatrix} 1 & 0.9 & 0.8 \\ 0.8 & 1 & 0.9 \\ 0.7 & 0.8 & 1 \end{pmatrix}. \text{ Afterwards, we consider all 4 sources, mixed by the}$$

$$\text{matrix } \mathbf{A} = \begin{pmatrix} 1 & 0.9 & 0.8 & 0.7 \\ 0.7 & 1 & 0.9 & 0.8 \\ 0.8 & 0.9 & 1 & 0.7 \\ 0.7 & 0.8 & 0.9 & 1 \end{pmatrix}. \text{ The parameters involved in the algorithms}$$

are chosen as in the previous subsection for the two methods. In the second method, we use a modified algorithm aiming at jointly diagonalizing several correlation matrices corresponding to several frequency shifts (which may be considered as a frequency equivalent of the SOBI algorithm). Figure 3 shows the mean and the standard deviation of SIR on 100 simulations using these two methods. It can be seen that the performance degrades when the number of sources increases, but it remains acceptable even with 4 sources.

## 5.3 Real-world sources

### 5.3.1 Results using the first method and telecom sources

Two real-world cyclo-stationary telecommunication signals were used for this experiment. The first signal is a recorded GMSK-modulated burst signal, used in the European digital cellular communication system, called GSM. The second signal is a very noisy QAM16-modulated signal. Both signals have been shifted to the central frequency 20 MHz and resampled at 80 million samples per second. The shifted signals and their power spectra are shown in Fig. 4.

9984 samples of these signals were artificially mixed using the mixing matrix

$\mathbf{A} = \begin{pmatrix} 1 & 0.9 \\ 0.8 & 1 \end{pmatrix}$ . Then, the algorithm of Section 3 was used for separating them. Note that each cyclo-stationarity period contains 4 samples of the mixtures. Thus, the 32-point Discrete Fourier Transforms were computed on each of 312 frames of 8 periods. The spectral expected values were estimated by averaging the spectral functions on these 312 frames. Following Theorem 3, the frequency  $\omega_1$  in the algorithm was chosen as half of the cyclo-stationarity frequency. The experiment led to a 41.8-dB SIR.

### 5.3.2 Results using the second method and speech sources

In another experiment, the second method, presented in Section 4, based on the frequency-version of the SOBI algorithm was used for separating mixtures of speech signals with a mixing matrix  $\mathbf{A} = \begin{pmatrix} 1 & 0.9 \\ 0.8 & 1 \end{pmatrix}$ . Five tests using five couples of 100000-sample speech signals led to an average SIR of 43.8 dB.

This experiment shows that although Theorem 4 is derived for temporally uncorrelated signals, the proposed method works well also for temporally correlated signals. Nevertheless, to satisfy rigorously the conditions of Theorem 4, we can use the approach for autocorrelated sources proposed at the end of Section 4, which allows us to obtain temporally uncorrelated observations. Applying a frequency-version of the SOBI algorithm to the observations resulting from this approach led to an average SIR of 48.1 dB.

Both versions of our method outperform all the 19 algorithms provided by ICALAB 2.2. The best results obtained with these algorithms were 43.1 dB (FPICA and PEARSON) and 43.0 dB (ERICA and UNICA).

### 5.3.3 Multi-tag radio-frequency identification

Many real-world situations require to identify people, animals or objects. This can be done using an electronic system based on radio-frequency (RF) communication [28]. It consists of a base station inductively coupled to portable identifiers (called *tags*) which contain an LC resonator, a controller and a non-volatile programmable memory (EEPROM). The memory contents are specific to each tag and allow to identify the tag bearer (person or object). The basic mode of operation of this system may be modeled as follows. The base station emits an RF sine wave, which is received by a single tag. The tag is thus powered and answers by emitting a sine wave at the same frequency

(due to inductive coupling), modulated by its encoded memory contents. The base station receives this signal, demodulates it, and decodes it so as to determine the memory contents. The overall identification system then checks these data and controls its actuators accordingly.

This type of system is attractive because it yields contactless operation between the base station and tags, and because it operates with battery-less tags. However, when two tags are placed in the RF field of the base station, both tags answer this station. The demodulated signal derived by this station is then a mixture of two components, and cannot be decoded by this basic station. This system is therefore unable to identify two simultaneously present tag bearers. A few attempts to solve this type of problem have been presented in the literature [29],[30]. In [28], we proposed to use an extension of the standard system described above. For simultaneously handling two tag signals, it relies on a base station containing two reception antennas and two demodulators, which yield two mixed signals. These mixed signals are processed by a BSS unit, which extracts the two components corresponding to the two tags. Then, by decoding these separated signals, the memory contents of the two tags are obtained independently. However, the methods considered in [28] were not efficient for data lengths smaller than 1000 samples.

In [28], it has been demonstrated that the assumption of linear instantaneous mixture is realistic. Since the sources are cyclo-stationary (as shown in [31]), we can apply the two methods proposed in the current paper for separating them. Evidently, the mixing matrix depends on the relative positions of the tag-bearers with respect to the station. To compare our results to those reported in [28], we consider the same following two mixing matrices corresponding

respectively to weakly mixed and highly mixed sources:  $\mathbf{A}_1 = \begin{pmatrix} 1 & 0.4 \\ 0.3 & 1 \end{pmatrix}$  and  $\mathbf{A}_2 = \begin{pmatrix} 1 & 0.98 \\ 0.98 & 1 \end{pmatrix}$ . In [28], instead of the SIR criterion (15), another criterion

called Signal to Interference Ratio Improvement (SIRI) has been used which is defined by:

$$SIRI = 0.5 \sum_{i=1}^2 10 \log_{10} \frac{E[(x_i - s_i)^2]}{E[(\hat{s}_i - s_i)^2]}, \quad (17)$$

In the following, we report our experimental results using both criteria. Fig. 5 shows SIR of our two methods as a function of sample size for the two mixing matrices mentioned above. Fig. 6 compares SIRI of our methods with those reported in [28]<sup>10</sup>. From these figures, it is clear that our methods outperform

<sup>10</sup> In [28], several nonlinear decorrelation-based algorithms are realized using neural networks. Here, we consider the results obtained using a recurrent neural network, called NWUr in [28].

those used in [28]. In particular, the algorithms used in [28] are not capable to separate the sources containing less than 900 samples while our methods provide quite good results even with 256 samples. The performance figures of our two methods are rather similar. Note also that SIR is almost independent from the mixing matrix so that the separation performance does not depend on the positions of tag-bearers. On the other hand, SIRI is a function of the mixing matrix because the numerator of the fraction in (17) is a function of the mixing matrix.

## 6 Conclusion

A major objective of this paper was to demonstrate and exploit some theoretically interesting frequency-domain properties of random signals which are non-stationary in the time domain. These properties provide sufficient second-order constraints in the frequency domain for separating linear instantaneous mixtures of non-stationary sources.

Two separating methods were proposed based on these properties. The first method is theoretically interesting but its implementation is difficult unless either many realizations of the mixtures are available or the sources are cyclostationary. The second method is very simple and powerful because it allows the second-order time-domain algorithms developed for stationary time-correlated signals to be applied to temporally uncorrelated sources which are non-stationary in the time domain, just by mapping them in the frequency domain. It should be remarked that these algorithms do not require the variance of the sources to be constant over subintervals, while this hypothesis is necessary in the majority of the source separation algorithms based on the non-stationarity of variance which have been reported in the literature.

Various test results using artificial and real-world sources confirmed the good performance of the proposed methods.

## Acknowledgments

The authors would like to thank Frédéric Abrard from i2e Télécom for providing the telecommunication signals used in the tests reported in Section 5.3.1.

## A Proof of Theorem 1

From (2), we have

$$\mathbf{Q}_X(\omega) = \mathbf{A}\mathbf{Q}_S(\omega)\mathbf{A}^T \quad (\text{A-1})$$

and

$$\mathbf{R}_X(\omega) = \mathbf{A}\mathbf{R}_S(\omega)\mathbf{A}^H = \mathbf{A}\mathbf{R}_S(\omega)\mathbf{A}^T \quad (\text{A-2})$$

because  $\mathbf{A}$  is real. If  $\mathbf{R}_S(\omega)$  is nonsingular, *i.e.* if  $E[|S_i(\omega)|^2] \neq 0 \forall i$ , then left multiplying (A-1) by the inverse of (A-2) yields

$$\mathbf{R}_X^{-1}(\omega)\mathbf{Q}_X(\omega) = \mathbf{A}^{T^{-1}}\mathbf{R}_S^{-1}(\omega)\mathbf{Q}_S(\omega)\mathbf{A}^T. \quad (\text{A-3})$$

Since, according to Corollary 1,  $\mathbf{R}_S^{-1}(\omega)\mathbf{Q}_S(\omega)$  is a diagonal matrix, the above equation is nothing but an eigenvalue decomposition of the matrix  $\mathbf{R}_X^{-1}(\omega)\mathbf{Q}_X(\omega)$ . If the  $K$  eigenvalues are distinct (*i.e.* if the algebraic multiplicity of each eigenvalue equals one), then the dimension of the eigenspace corresponding to each eigenvalue equals one (see [18]-page 58). In other words, if  $\mathbf{v}$  and  $\mathbf{u}$  are two eigenvectors corresponding to the same eigenvalue  $\lambda$ , then  $\mathbf{u} = \alpha\mathbf{v}$  where  $\alpha$  is a (complex) scalar. Moreover, it is clear that the eigenvalues may be arranged as diagonal entries of a diagonal matrix in an arbitrary order.

Hence, if the matrix  $\mathbf{R}_X^{-1}(\omega)\mathbf{Q}_X(\omega)$  has  $K$  distinct eigenvalues (which are the diagonal entries of  $\mathbf{R}_S^{-1}(\omega)\mathbf{Q}_S(\omega)$ ), *i.e.* if  $\frac{E[S_i^2(\omega)]}{E[|S_i(\omega)|^2]} \neq \frac{E[S_j^2(\omega)]}{E[|S_j(\omega)|^2]} \forall i \neq j$ , and if  $\mathbf{V}\mathbf{\Lambda}\mathbf{V}^{-1}$  is an eigenvalue decomposition of  $\mathbf{R}_X^{-1}(\omega)\mathbf{Q}_X(\omega)$ , then the columns of  $\mathbf{V}$  are equal to the columns of  $\mathbf{A}^{T^{-1}}$  up to a scaling factor and a permutation, so that  $\mathbf{V} = \mathbf{A}^{T^{-1}}\mathbf{D}\mathbf{P}_1$ , where  $\mathbf{D}$  is a diagonal matrix and  $\mathbf{P}_1$  is a permutation matrix. It follows that  $\mathbf{V}^T = \mathbf{P}_1^T\mathbf{D}^T\mathbf{A}^{-1} = \mathbf{P}\mathbf{D}\mathbf{A}^{-1}$ . Note that  $\mathbf{P} = \mathbf{P}_1^T$  is a permutation matrix too.

Conversely, if  $\lambda = \frac{E[S_i^2(\omega)]}{E[|S_i(\omega)|^2]} = \frac{E[S_j^2(\omega)]}{E[|S_j(\omega)|^2]}$  for  $i \neq j$ , then  $\mathbf{R}_X^{-1}(\omega)\mathbf{Q}_X(\omega)$  has two identical eigenvalues  $\lambda$ . Since  $\mathbf{A}$  is supposed nonsingular, the columns of  $\mathbf{A}^{T^{-1}}$  (which represent the eigenvectors of  $\mathbf{R}_X^{-1}(\omega)\mathbf{Q}_X(\omega)$ ) are linearly independent. Hence, the eigenspace corresponding to  $\lambda$ , and spanned by two columns of  $\mathbf{A}^{T^{-1}}$ , is of dimension 2. It is well known that every nonzero element of this eigenspace is an eigenvector corresponding to  $\lambda$  (see [18]-section 1.4). Therefore, the two columns of  $\mathbf{A}^{T^{-1}}$  corresponding to  $\lambda$  cannot be identified up to a permutation and a scaling factor using the eigenvalue decomposition (5).

## B Proof of Theorem 3

From the definition of the discrete-time Fourier transform, it follows that

$$E[S^2(\omega)] = \sum_{n_1=-\infty}^{\infty} \sum_{n_2=-\infty}^{\infty} E[s(n_1)s(n_2)]e^{-j\omega(n_1+n_2)}. \quad (\text{B-1})$$

Since  $s(n)$  is cyclo-stationary with period  $N_c$ , its autocorrelation is periodic on the diagonal of the  $(n_1, n_2)$  plane with period  $N_c$  (supposed integer) so that we can write

$$E[S^2(\omega)] = \sum_{n_1=-\infty}^{\infty} \sum_{n_2=-\infty}^{\infty} E[s(n_1 + N_c)s(n_2 + N_c)]e^{-j\omega(n_1+n_2)}. \quad (\text{B-2})$$

Using the new variables  $m_1 = n_1 + N_c$  and  $m_2 = n_2 + N_c$ , the above equation can be rewritten as

$$E[S^2(\omega)] = \sum_{m_1=-\infty}^{\infty} \sum_{m_2=-\infty}^{\infty} E[s(m_1)s(m_2)]e^{-j\omega(m_1-N_c+m_2-N_c)}. \quad (\text{B-3})$$

It follows that

$$E[S^2(\omega)] = E[S^2(\omega)]e^{j2\omega N_c} \quad (\text{B-4})$$

which can be rewritten as

$$E[S^2(\omega)](1 - e^{j2\omega N_c}) = 0. \quad (\text{B-5})$$

Hence, the only frequencies at which  $E[S^2(\omega)]$  may be nonzero are the solutions of  $e^{j2\omega N_c} = 1$ , *i.e.*  $\omega = k\pi/N_c = k\omega_c/2$  where  $k$  is an integer.

## C Proof of Theorem 6

Consider the vector  $\tilde{\mathbf{s}}(n) = [\tilde{s}_1(n), \dots, \tilde{s}_K(n)]^T$ . Since  $\tilde{\mathbf{s}}(n) = z(n)\mathbf{s}(n)$ , we have

$$E[\tilde{\mathbf{s}}(n_1)\tilde{\mathbf{s}}^T(n_2)] = E[z(n_1)z(n_2)\mathbf{s}(n_1)\mathbf{s}^T(n_2)]$$

Because  $z(n)$  is stationary, temporally uncorrelated and independent from all the sources  $s_i(n)$ , we can write

$$E[\tilde{\mathbf{s}}(n_1)\tilde{\mathbf{s}}^T(n_2)] = \sigma_z^2\delta(n_1 - n_2)E[\mathbf{s}(n_1)\mathbf{s}^T(n_2)] \quad (\text{C-1})$$

where  $\sigma_z^2$  is the power of  $z(n)$ . Since  $E[\mathbf{s}(n_1)\mathbf{s}^T(n_2)]$  is a diagonal matrix,  $E[\tilde{\mathbf{s}}(n_1)\tilde{\mathbf{s}}^T(n_2)]$  is diagonal too, so that the new sources  $\tilde{s}_i(n)$  are mutually uncorrelated too.

Equation (C-1) implies

$$E[\tilde{s}_i(n_1)\tilde{s}_i(n_2)] = \sigma_z^2 \delta(n_1 - n_2) E[s_i(n_1)s_i(n_2)] = \sigma_z^2 \delta(n_1 - n_2) E[s_i^2(n_1)] \quad (\text{C-2})$$

Thus, the new sources  $\tilde{s}_i(n)$  are temporally uncorrelated. Moreover, taking  $n = n_1 = n_2$  in (C-2), we obtain  $E[\tilde{s}_i^2(n)] = \sigma_z^2 E[s_i^2(n)]$  so that the *normalized* variance profiles of  $\tilde{s}_i(n)$  and  $s_i(n)$  are equal.

## D Derivation of Equations (14)

The autocorrelation functions of  $s_1(n)$  and  $s_2(n)$  are

$$\begin{aligned} E[s_1(n_1)s_1(n_2)] &= 4 \cos(\omega_0 n_1) \cos(\omega_0 n_2) \delta(n_1 - n_2) = 4 \cos^2(\omega_0 n_1) \delta(n_1 - n_2) \\ &= (2 + 2 \cos(2\omega_0 n_1)) \delta(n_1 - n_2) \\ E[s_2(n_1)s_2(n_2)] &= 4 \sin(\omega_0 n_1) \sin(\omega_0 n_2) \delta(n_1 - n_2) = 4 \sin^2(\omega_0 n_1) \delta(n_1 - n_2) \\ &= (2 - 2 \cos(2\omega_0 n_1)) \delta(n_1 - n_2) \end{aligned} \quad (\text{D-1})$$

Hence,

$$\begin{aligned} E[S_1^2(\omega)] &= \sum_{n_1=-\infty}^{\infty} \sum_{n_2=-\infty}^{\infty} E[s_1(n_1)s_1(n_2)] e^{-j(n_1+n_2)\omega} \\ &= \sum_{n_1=-\infty}^{\infty} \sum_{n_2=-\infty}^{\infty} (2 + 2 \cos(2\omega_0 n_1)) \delta(n_1 - n_2) e^{-j(n_1+n_2)\omega} \\ &= \sum_{n_1=-\infty}^{\infty} (2 + 2 \cos(2\omega_0 n_1)) e^{-j2n_1\omega} \\ &= 2\pi \sum_{l=-\infty}^{\infty} 2\delta(2\omega - 2l\pi) + \delta(2\omega - 2\omega_0 - 2l\pi) + \delta(2\omega + 2\omega_0 - 2l\pi) \end{aligned} \quad (\text{D-2})$$

The same approach may be used to compute  $E[S_2^2(\omega)]$ .

We now show that this result is consistent with Theorem 3. The cyclo-stationarity frequency of the sources  $s_1(n)$  and  $s_2(n)$  is  $\omega_c = 2\omega_0$  because due to (D-1)

$$E[s_i(n_1)s_i(n_2)] = (2 \pm 2 \cos(2\omega_0 n_1)) \delta(n_1 - n_2) = E[s_i(n_1 + \frac{2\pi}{2\omega_0})s_i(n_2 + \frac{2\pi}{2\omega_0})] \quad i = 1, 2.$$

Replacing  $k$  in Theorem 3 by  $l\frac{\pi}{\omega_0}$ ,  $l\frac{\pi}{\omega_0} + 1$ , and  $l\frac{\pi}{\omega_0} - 1$  for integer values of  $l$ , we obtain all the frequency components of (D-2). Note that the cyclo-stationarity period  $N_c = \frac{2\pi}{\omega_c} = \frac{\pi}{\omega_0}$  is supposed to be integer for a discrete-time signal.

## E Derivation of Equations (16)

Considering (D-1), we have for the real signal  $s_1(n)$

$$\begin{aligned}
 E[S_1(\omega + v)S_1^*(\omega)] &= \sum_{n_1=-\infty}^{\infty} \sum_{n_2=-\infty}^{\infty} E[s_1(n_1)s_1(n_2)]e^{-j(\omega+v)n_1}e^{j\omega n_2} \\
 &= \sum_{n_1=-\infty}^{\infty} \sum_{n_2=-\infty}^{\infty} (2 + 2\cos(2\omega_0 n_1))\delta(n_1 - n_2)e^{-j(\omega+v)n_1}e^{j\omega n_2} \\
 &= \sum_{n_1=-\infty}^{\infty} (2 + 2\cos(2\omega_0 n_1))e^{-jvn_1} \\
 &= 2\pi \sum_{l=-\infty}^{\infty} 2\delta(v - 2l\pi) + \delta(v - 2\omega_0 - 2l\pi) + \delta(v + 2\omega_0 - 2l\pi)
 \end{aligned}$$

The same approach may be used to compute  $E[S_2(\omega + v)S_2^*(\omega)]$ .

## References

- [1] J.-F. Cardoso, The three easy routes to independent component analysis: contrast and geometry, in *Proc. ICA2001*, San Diego, 2001, pp. 1-6.
- [2] A. Cichocki, S.-I. Amari, *Adaptive blind signal and image processing - learning algorithms and applications*, Wiley, New York, 2002.
- [3] K. Matsuoka, M. Ohya, Mitsuru Kawamoto, A neural net for blind separation of non-stationary signals, *Neural Networks*, vol. 8, no. 3, pp. 411-419, 1995.
- [4] S. Choi, A. Cichocki, S. Amari, Equivariant non-stationary source separation, *Neural Networks*, vol. 15, no. 1, pp. 121-130, Jan. 2002.
- [5] A. Souloumiac, Blind source detection and separation using second-order non-stationarity, in *Proc. ICASSP*, 1995, pp. 1912-1915.
- [6] S. Choi, A. Cichocki, A. Belouchrani, Second order non-stationary source separation, *Journal of VLSI Signal Processing*, vol. 32, no. 1-2, pp. 93-104, Aug. 2002.
- [7] A. Hyvarinen, Blind source separation by non-stationarity of variance: a cumulant based approach, *IEEE Trans. on Neural Networks*, vol. 12, no. 6, pp. 1471-1474, 2001.
- [8] D.-T. Pham, J.-F. Cardoso, Blind separation of independent mixtures of non-stationary sources, *IEEE Trans. on Signal Processing*, vol. 49, no. 9, 2001.
- [9] L. Parra, C. Spence, Convolutional blind separation of non-stationary sources, *IEEE Trans. on Speech and Audio Processing*, vol. 8, no. 3, 2000.



- [10] A. Belouchrani, M. G. Amin, Blind source separation based on time-frequency signal representation, *IEEE Trans. on Signal Processing*, vol. 46, no. 11, November 1998.
- [11] F. Abrard, Y. Deville, P. White, From blind source separation to blind source cancellation in the underdetermined case: a new approach based on time-frequency analysis, in *Proc. ICA2001*, pp. 734-739, San Diego, USA, 2001.
- [12] Y. Deville, Temporal and time-frequency correlation-based blind source separation methods, in *Proc. ICA2003*, pp. 1059-1064, Nara, Japan, 2003.
- [13] F. Abrard, Y. Deville, A time-frequency blind signal separation method applicable to underdetermined mixtures of dependent sources, *Signal Processing*, vol. 85, no. 7, pp. 1389-1403, July 2005.
- [14] D. Nuzillard, J.-M. Nuzillard, Second-order blind source separation in the Fourier space of data, *Signal Processing*, vol. 83, no. 3, pp. 627-631, March 2003.
- [15] A. Papoulis, S. U. Pillai, *Probability, random variables and stochastic processes*, 4th Ed., McGraw-Hill, 2002.
- [16] J. Eriksson, V. Koivunen, Complex random vectors and ICA models: identifiability, uniqueness, and separability, *IEEE Trans. on Information Theory*, vol. 52, no. 3, pp. 1017-1029, March 2006.
- [17] L. Tong, R.-W. Liu, V. C. Soon, Y.-F. Huang, Indeterminacy and identifiability of blind identification, *IEEE Trans. Circuits Syst.*, vol. 38, no. 5, pp. 499-509, May 1991.
- [18] R. A. Horn, C. R. Johnson, *Matrix analysis*, Cambridge University Press, 1999.
- [19] W. A. Gardner, W. A. Brown, C. K. Chen, Spectral correlation of modulated signals: Part II-Digital modulations, *IEEE Trans. Commun.*, vol. COMM-35, June 1987.
- [20] A. Ferréol, P. Chevalier, On the behavior of current second and higher order blind source separation methods for cyclo-stationary sources, *IEEE Trans. on Signal Processing*, vol. 48, pp. 1712-1725, June 2000. Erratum: vol 50, pp. 990, Apr. 2002.
- [21] K. Abed-Meraim, Y. Xiang, J. H. Manton, Y. Hua, Blind source separation using second-order cyclo-stationary statistics, *IEEE Trans. on Signal Processing*, vol. 49, pp. 694-701, Apr. 2001.
- [22] A. Ferréol, P. Chevalier, L. Albera, Second-order blind separation of first- and second-order cyclo-stationary sources-application to AM, FSK, CPFSK, and deterministic sources, *IEEE Trans. on Signal Processing*, vol. 52, no. 4, pp. 845-861, Apr. 2004.
- [23] M. Mazet, P. Loubaton, Estimation de la période symbole d'un signal modulé linéairement basée sur des cyclo-corrélations, in *Proc. GretsI*, Vannes, France, Sept. 1999.

- [24] A. Belouchrani, K. Abed Meraim, J.-F. Cardoso, E. Moulines, A blind source separation technique based on second order statistics, *IEEE Trans. on Signal Processing*, vol. 45, pp. 434-444, Feb. 1997.
- [25] S. Degerine, R. Malki, Second order blind separation of sources based on canonical partial innovations, *IEEE Trans. on Signal Processing*, vol. 48, pp. 629-641, 2000.
- [26] S. Hosseini, C. Jutten, D.-T. Pham, Markovian source separation, *IEEE Trans. on Signal Processing*, vol. 51, no. 12, pp. 3009-3019, Dec. 2003.
- [27] A. Cichocki, S. Amari, K. Siwek, T. Tanaka et al., *ICALAB Toolboxes*, <http://www.bsp.brain.riken.jp/ICALAB>.
- [28] Y. Deville, J. Damour, N. Charkani, Multi-tag radio-frequency identification systems based on new blind source separation neural networks, *Neurocomputing* (49), pp. 369-388, 2002.
- [29] P.-R.-M. Denne, C.-D. Hook, Identification Systems, *UK patent no. 2 157 132 A*, 16 Oct. 1985.
- [30] C.-D. Hook, C.-S. Hall, Transponder system, *European patent no. 0 527 172 B1*, 5 Apr. 1995.
- [31] H. Saylani, Y. Deville, S. Hosseini, M. Habibi, A Multi-tag radio-frequency identification system using a new blind source separation method based on spectral decorrelation, in *Proceedings of ISCCSP'2006: 2nd Int. Symp. On Communications, Control, and Signal Processing*, pp. 44-48, Marrakech, Morocco, Mars 2006.

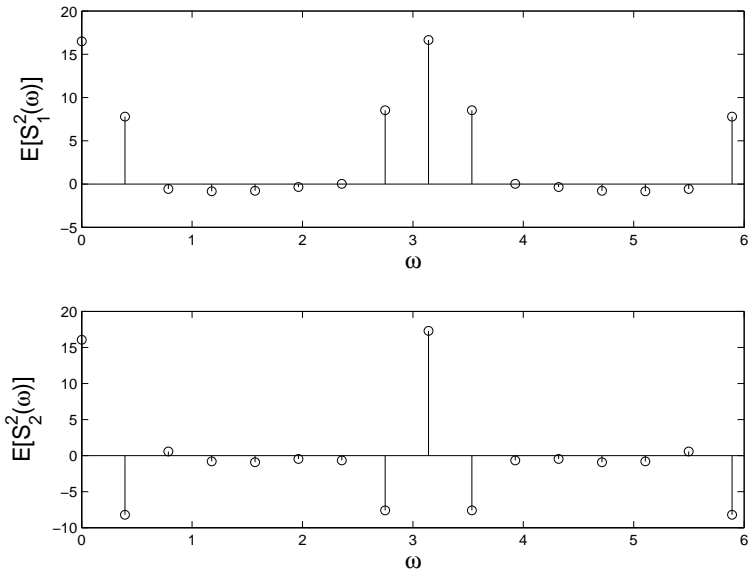


Fig. 1. Estimates of  $E[S_1^2(\omega)]$  and  $E[S_2^2(\omega)]$  for the sources used in simulations.

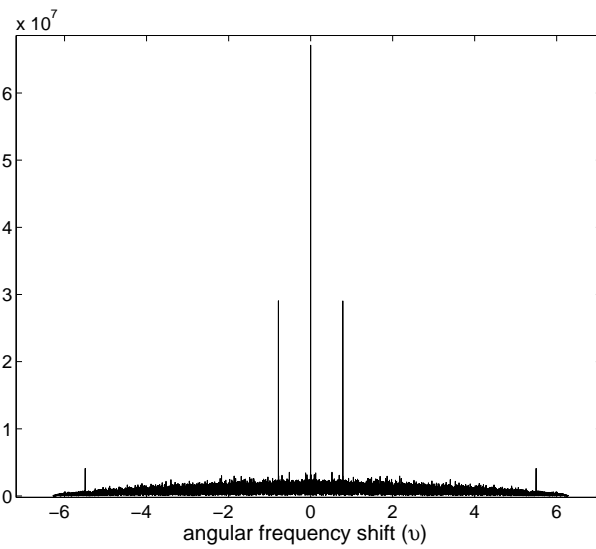


Fig. 2. Estimate of autocorrelation function of  $S_1(\omega)$ .

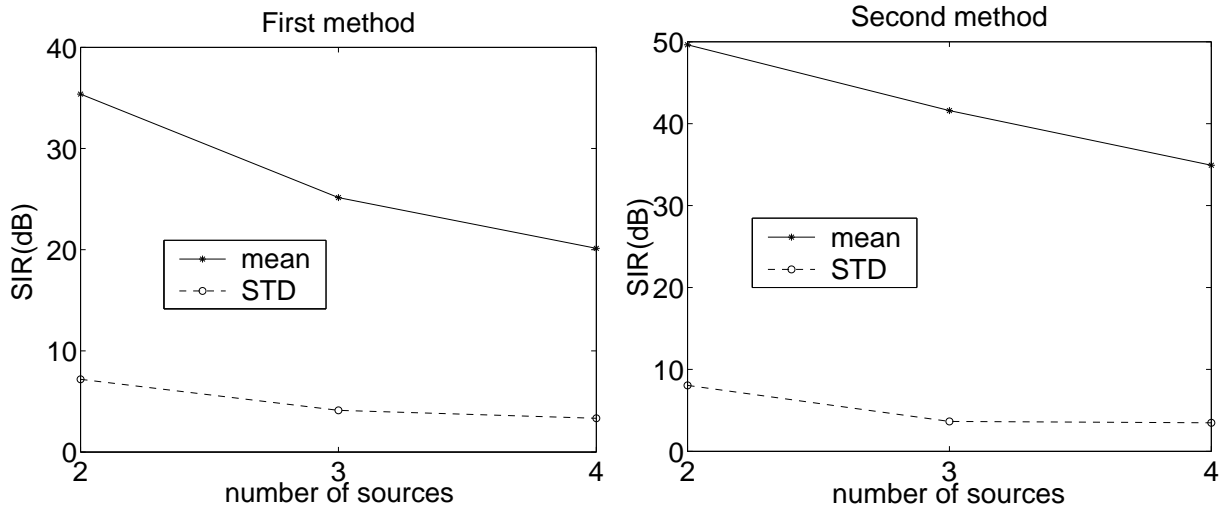


Fig. 3. SIR as a function of number of artificial sources.

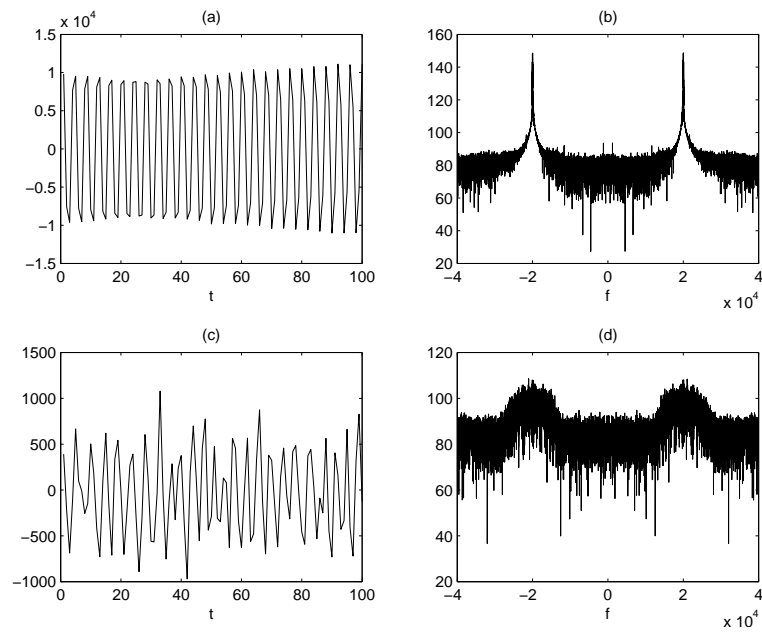


Fig. 4. Telecommunication sources: (a) zoom of first signal, (b) its complete power spectrum, (c) zoom of second signal, (d) its complete power spectrum.

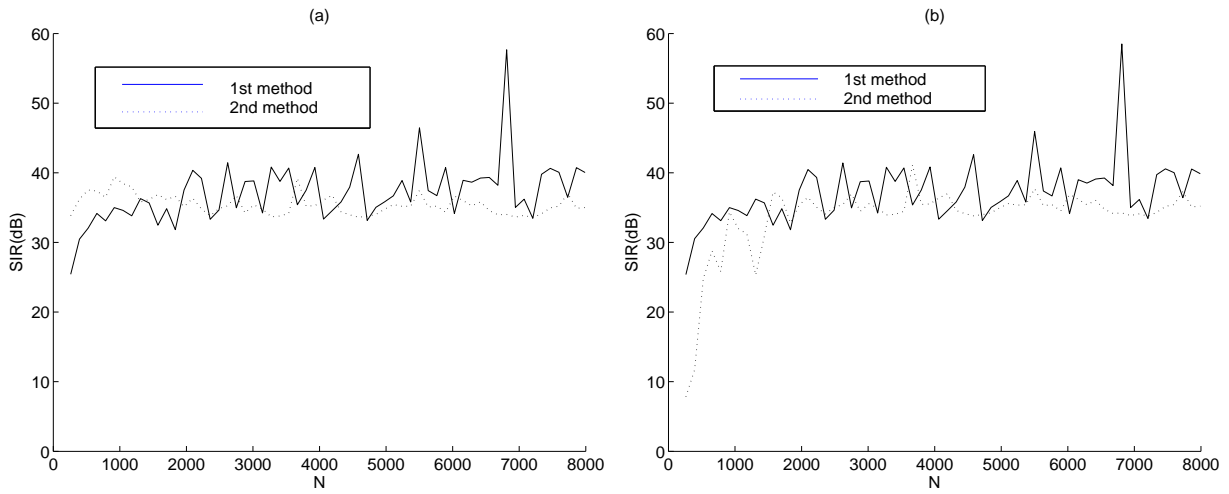


Fig. 5. SIR of our methods used for multi-tag identification versus number  $N$  of samples: (a) weakly mixed sources, (b) highly mixed sources.

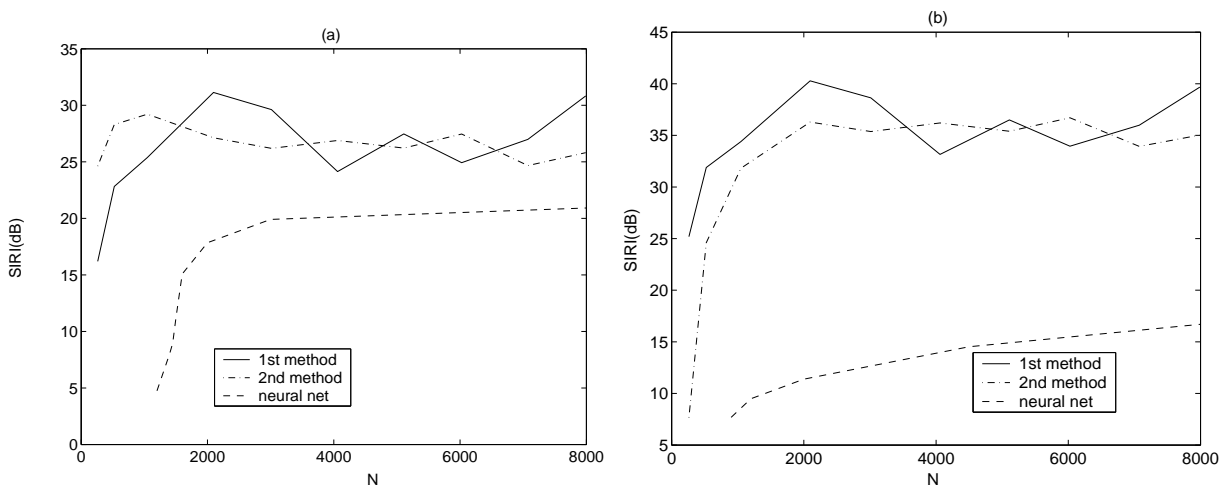


Fig. 6. SIRI of our methods and recurrent neural network-based method reported in [28] used for multi-tag identification versus number  $N$  of samples: (a) weakly mixed sources, (b) highly mixed sources.